4598–4608 *Nucleic Acids Research, 1999, Vol. 27, No. 23*

Spb1p is a putative methyltransferase required for 60S ribosomal subunit biogenesis in *Saccharomyces cerevisiae*

Dieter Kressler, Manuel Rojo[1], Patrick Linder and Jesús de la Cruz*

Département de Biochimie Médicale, Centre Médical Universitaire, Université de Genève, 1 rue Michel-Servet, 1211 Genève 4, Switzerland and [1]INSERM U523–Institut de Myologie, Groupe Hospitalier Pitié-Salpêtrière, 47 boulevard de l'Hôpital, 75651 Paris Cedex 13, France

Received August 10, 1999; Revised and Accepted October 19, 1999

ABSTRACT

Several mutants (*spb1–spb7*) have been previously identified as cold-sensitive extragenic suppressors of loss-of-function mutations in the poly(A)$^+$-binding protein 1 of *Saccharomyces cerevisiae*. Cloning, sequence and disruption analyses revealed that *SPB1* (YCL054W) encodes an essential putative *S*-adenosylmethionine-dependent methyltransferase. Polysome analyses showed an under-accumulation of 60S ribosomal subunits in the *spb1-1* mutant and in a strain genetically depleted of Spb1p. Northern and primer extension analyses indicated that this was due to inhibition of processing of the 27SB precursors, which results in depletion of the mature 25S and 5.8S rRNAs. At later time points of Spb1p depletion, the stability of 40S ribosomal subunits is also affected. These results suggest that Spb1p is involved in 60S ribosomal subunit biogenesis and associates early with the pre-ribosomes. Consistent with this, hemagglutinin epitope-tagged Spb1p localizes to the nucleus with nucleolar enrichment. Despite the expected methyltransferase activity of Spb1p, global methylation of pre-rRNA is not affected upon Spb1p depletion. We propose that Spb1p is required for proper assembly of pre-ribosomal particles during the biogenesis of 60S ribosomal subunits.

INTRODUCTION

The synthesis of ribosomes is one of the major cellular activities that, in eukaryotes, takes place primarily in a specialized subnuclear compartment termed the nucleolus (1,2). The basic outline of ribosome synthesis is conserved throughout eukaryotes, however, most of our knowledge comes from the combination of molecular genetic and biochemical approaches in the yeast *Saccharomyces cerevisiae* (reviewed in 3–5).

In *S.cerevisiae*, three of the four rRNAs (18S, 5.8S and 25S) are transcribed as a single large pre-rRNA by RNA polymerase I (RNA pol I), whereas the fourth rRNA (5S) is independently transcribed as a pre-rRNA by RNA polymerase III (3,4,6). In the 35S pre-rRNA, which is the longest detectable precursor, the mature rRNA sequences are separated by two internal transcribed spacer sequences, ITS1 and ITS2, and flanked by two external transcribed spacer sequences, 5′-ETS and 3′-ETS (Fig. 1). Processing of the 35S pre-rRNA is a fairly well-characterized multistep pathway that requires many different *trans*-acting factors (Fig. 1B and its legend), including small nucleolar RNAs (snoRNAs), nucleolar ribonucleoprotein particles (snoRNPs), endo- and exonucleases and putative ATP-dependent RNA helicases (reviewed in 7–12).

Mainly shortly after transcription, many specific nucleotides within the rRNA undergo covalent modification. These modifications include isomerization of uridine to pseudouridine (Ψ) by base rotation (pseudouridylation; 45 modified nucleotides), methylation of the 2′-hydroxyl group of sugar residues (2′-*O*-ribose methylation; 55 modified nucleotides) and base methylation (~10 modified nucleotides) (13–15). H/ACA-box snoRNPs are required for pseudouridylation, whereas C/D-box snoRNPs are required for 2′-*O*-ribose methylation (16–18). Cbf5p, which is an integral component of H/ACA-box snoRNPs, is most likely the rRNA Ψ-synthase (19,20), however, the 2′-*O*-ribose methylase(s) has not yet been identified. Little is known about base methylation in eukaryotes and, in contrast to Ψ formation and 2′-*O*-ribose methylation, it does not appear to involve guide snoRNAs. The only base methylation studied in yeast is the dimethylation of two adjacent adenosines ($m^{6,2}A_{1779}$ and $m^{6,2}A_{1780}$) at the 3′-end of 18S rRNA. This reaction is catalyzed by the essential dimethylase Dim1p (21–23).

In clear contrast to the pre-rRNA processing pathway, the assembly process of the rRNAs and ribosomal proteins (r proteins) into mature ribosomal subunits is still poorly understood. In the nucleolus, the pre-rRNAs associate with many of the r-proteins to form pre-ribosomal particles (24). In addition to r-proteins, the pre-ribosomes have long been known to contain non-r-proteins (24). The identity of these proteins has not been clearly established, but they most likely correspond to *trans*-acting factors that are required for pre-rRNA processing and modification or are involved in the assembly of the pre-rRNAs with the r-proteins (see for example 25).

We are interested in the identification and functional characterization of new *trans*-acting factors involved in yeast ribosome

*To whom correspondence should be addressed at present address: Instituto de Bioquímica Vegetal y Fotosíntesis, Centro de Investigaciones Científicas Isla de la Cartuja, Avenida Américo Vespucio s/n, Isla de la Cartuja, E-41092 Sevilla, Spain. Tel: +34 95 4489519; Fax: +34 95 4460065; Email: jdlcd@cica.es

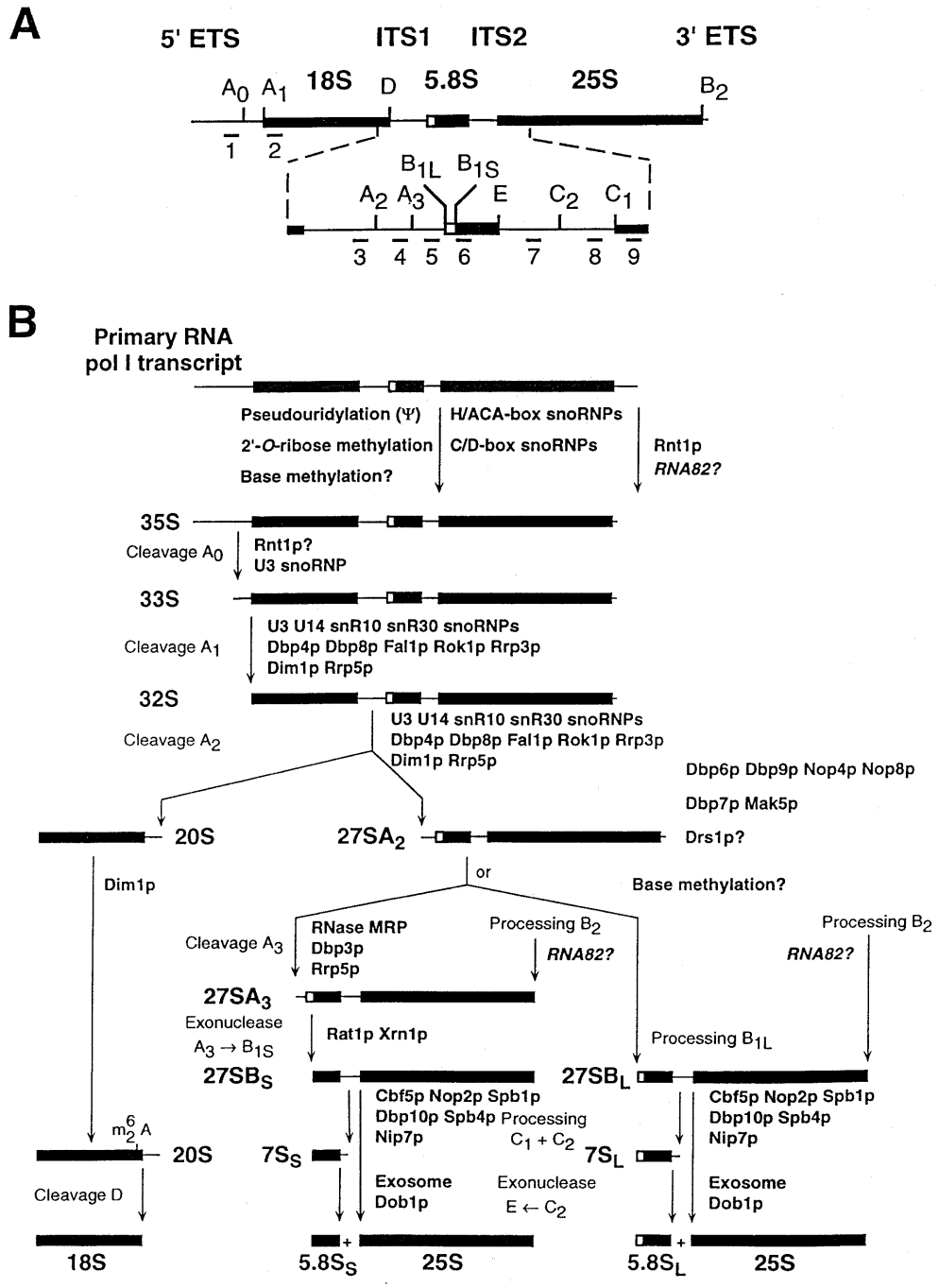

Figure 1. Pre-rRNA processing in *S.cerevisiae*. (**A**) Structure of the 35S pre-rRNA and processing sites. This precursor contains the sequences for the mature 18S, 5.8S and 25S rRNAs that are separated by the two internal transcribed spacers ITS1 and ITS2, and flanked by two external transcribed spacers, 5′-ETS and 3′-ETS. The location of various probes (numbered 1–9) used in this study are indicated. Bars represent mature rRNA species and lines the transcribed spacers. (**B**) Pre-rRNA processing pathway. The primary RNA polymerase I transcript is processed at its 3′-end to yield the 35S pre-rRNA, which is the longest detectable pre-rRNA. Pseudouridylation and 2′-*O*-ribose methylation take place on the primary transcript (57,61). Note that except for Dim1p, timing of and *trans*-acting factors involved in base methylation have not yet been uncovered. The 35S pre-rRNA is first processed at sites A_0, A_1 and A_2, which results in the separation of the pre-rRNAs destined for the small and large ribosomal subunits. The 20S pre-rRNA is matured by endonucleolytic cleavage at site D. The $27SA_2$ precursor is processed by two alternative pathways. In the major pathway, ~85% of $27SA_2$ pre-rRNA is cleaved at site A_3. The $27SA_3$ pre-rRNA is further exonucleolytically 5′→3′ digested to site B_{1S}. In the minor pathway, ~15% of the $27SA_2$ molecules are processed at site B_{1L}. While processing at site B_1 is completed, the 3′-end of mature 25S rRNA is generated by processing at site B_2. The subsequent ITS2 processing of both 27SB species appears to be identical. Cleavage at sites C_1 and C_2 releases the mature 25S rRNA and the 7S pre-rRNA. The latter undergoes 3′→5′ exonucleolytic digestion to the 3′-end of mature 5.8S rRNA. The structural rearrangements within early or intermediate pre-ribosomal particles are likely to require the putative ATP-dependent RNA helicases Dbp6p, Dbp7p, Dbp9p and Drs1p (10), as well as the nucleolar proteins Nop4p (63,64) and Nop8p (65). The data presented in this study suggest that Spb1p, a putative S-AdoMet-dependent methyltransferase, is required for a late step in the assembly of 60S ribosomal subunits, a process that may also involve Nop2p, which is another putative S-AdoMet-dependent methyltransferase (55), Cbf5p, the putative Ψ-synthase (19), Nip7p (54) and the two putative ATP-dependent RNA helicases Dbp10p and Spb4p (10). For reviews on pre-rRNA processing and *trans*-acting factors see Venema and Tollervey (7,11) and Kressler *et al.* (12).

biogenesis. One class of proteins that are likely to be involved in this process are encoded by the *SPB* [suppressor of poly(A)$^+$-binding protein Pab1p] genes (26), because all described *spb* mutants, except *spb8* (27) and *pbp1* (28), show decreased steady-state levels of free 60S ribosomal subunits (26). Consistent with a role of the Spb proteins in the biogenesis of 60S ribosomal subunits, Spb2p is the r-protein Rpl39p (formerly L46) (26,29) and Spb4p is a putative ATP-dependent RNA helicase required for a late step in the assembly of 60S ribosomal subunits (25,29). The remaining *SPB* genes have so far not been identified. Moreover, it is still unclear how mutations in factors involved in 60S ribosomal subunit biogenesis can bypass the loss-of-function of Pab1p, which is required for translation initiation (26).

Herein, we report on the molecular cloning of the *SPB1* gene by complementation of the slow growth (sg$^-$) phenotype of the *spb1-1* mutant. Our results indicate that *SPB1* encodes an essential putative *S*-adenosylmethionine (S-AdoMet)-dependent methyltransferase that has been previously identified in a screen for genes involved in silencing and provisionally named *YCL54* (30). Spb1p localizes to the nucleus with nucleolar enrichment. Both, the *spb1-1* mutation and *in vivo* depletion of Spb1p result in a deficit in 60S ribosomal subunits. In the Spb1p-depleted strain, this deficit is likely to be the consequence of impaired production of mature 25S and 5.8S rRNAs due to the accumulation of 27SB pre-rRNAs. Nevertheless, global rRNA methylation is not affected upon Spb1p depletion. We conclude that Spb1p is required for the normal assembly of pre-ribosomal particles during the biogenesis of 60S ribosomal subunits.

MATERIALS AND METHODS

Strains, media and microbiological methods

The *S.cerevisiae* strains in this study are derivatives of the diploid strain W303 (MAT**a**/MATα *ura3-1*/*ura3-1 ade2-1*/*ade2-1 his3-11,15*/*his3-11,15 leu2-3,112*/*leu2-3,112 trp1-1*/*trp1-1*) (31). JDY9-1A (MATα *spb1-1*) and JDY9-2A (MAT**a** *spb1-1*) were obtained by introducing the *spb1-1* mutation from YAS151 (MATα *spb1-1 his3 leu2 trp1 ura3*) (26) into the W303 background by three subsequent back-crosses with ASZ1 (MAT**a** *ura3-1 ade2-1 his3-11,15 leu2-3,112 trp1-1*) (32). YDK14 (MAT**a**/MATα *spb1*::HIS3MX6/*SPB1*) was obtained by disrupting one *SPB1* ORF copy with the HIS3MX6 marker module in the diploid strain W303. YDK14-1A (MATα *spb1*::HIS3MX6) and YDK14-2C (MAT**a** *spb1*::HIS3MX6) are meiotic segregants of YDK14 that require a plasmid-borne copy of *SPB1* for cell viability. Preparation of standard media and genetic manipulations were according to established procedures (33,34). Yeast cells were transformed using a lithium acetate method (35). One-step gene replacements were done according to Wach *et al.* (36). For tetrad dissection, a Singer MSM micromanipulator was used. *Escherichia coli* DH10B was used for all recombinant DNA techniques (37). Plasmid rescue from yeast into *E.coli* was performed as described (38).

Cloning of *SPB1*

The sg$^-$ and cold-sensitive (cs$^-$) strain JDY9-1A was transformed with a pSEY18 (2μ-URA3)-based yeast genomic library, kindly provided by M. Hall (Biozentrum, University of Basel, Switzerland), and transformants were selected on SD-Ura plates at 30°C. One out of 30 000 Ura3$^+$ transformants displayed wild-type growth at 18 and 30°C. After plasmid rescue, this clone (pSEY18-SPB1) was able to reproducibly complement the sg$^-$ and cs$^-$ phenotype when back-transformed into JDY9-1A. Sequencing of pSEY18-SPB1 revealed that it contained an insert of 8.67 kb from chromosome III that included the complete open reading frames (ORFs) YCL054W and YCL052C (*PBN1*) and the almost complete ORF YCL055W (*KAR4*). Subcloning of a 5.48 kb *Spe*I–*Sac*I fragment from pSEY18-SPB1 into the *Xba*I + *Sac*I-restricted plasmid YCplac111 (*CEN-LEU2*) (39), yielding plasmid YCplac111-SPB1 (pDK403), indicated that the presence of ORF YCL054W (hereafter designated *SPB1*) was sufficient to complement the sg$^-$ and cs$^-$ phenotype of JDY9-1A. To confirm that YCL054W was indeed the *spb1* complementing gene, the YCL054W ORF, including 429 bp of the promoter and 309 bp of the terminator region, was PCR amplified (Vent polymerase; New England Biolabs) from YCplac111-SPB1 with oligonucleotides introducing the restriction sites *Sal*I (ODK105, 5′-GCA CGC GTC GAC CCA GAA ATA ATC GAA AGC AT-3′, *Sal*I site underlined) and *Sac*I (ODK108, 5′-GCA CGC GAG CTC CCA ATT CCA AGG CCT GAC A-3′, *Sac*I site underlined), respectively. The 3.26 kb PCR product was digested with *Sal*I and *Sac*I and cloned into the *Sal*I + *Sac*I-restricted vector pRS416 (*CEN-URA3*) (40) to yield plasmid pRS416-SPB1 (pDK343). This plasmid complemented the *spb1* null allele (see below) to the wild-type extent at 18, 30 and 37°C, and it complemented the sg$^-$ and cs$^-$ phenotype imposed by the *spb1-1* mutation.

Disruption of *SPB1*

A deletion disruption of the *SPB1* ORF was obtained by transformation of a PCR-synthesized HIS3MX6 marker cassette with short flanking homology regions (SFH-PCR) into W303 (36). Briefly, the heterologous HIS3MX6 marker module flanked on each side by short regions of homology to the *SPB1* locus was generated by PCR using plasmid pFA6a-HIS3MX6 (36) as the DNA template and the two oligonucleotides ODK103 (SFH5′) (5′-AGT TTG TAG TTA GAT TTA ACT CAA TAG AGG TGA TTG GCA AAA **ATG** CGT ACG CTG CAG GTC GAC3′, *SPB1* 5′ upstream sequence, with the start codon in bold type, underlined and the 5′ homology sequence to the HIS3MX6 marker module in plain type) and ODK104 (SFH3′) (5′-AGT AAT CTT GGG TCC AGC CTC TTT GGT GCC TTG AAA CCT TTA CAC ATC GAT GAA TTC GAG CTC G-3′, reverse complement of the *SPB1* coding sequence, with the deletion ending 1930 nt upstream of the stop codon, underlined and the 3′ homology sequence to the HIS3MX6 marker module in plain type). The SFH-PCR product was phenol extracted, concentrated by ethanol precipitation and then used to transform W303. Four His$^+$ transformants were examined by Southern analysis to confirm that integration had occurred at the *SPB1* genomic locus. One disrupted strain, YDK14, was sporulated and tetrads were dissected. In addition, YDK14 was transformed with pRS416-SPB1 or YCplac111-SPB1 and subjected to tetrad analysis. The two His$^+$ haploid segregants, YDK14-1A (MATα *spb1*::HIS3MX6) and YDK14-2C (MAT**a** *spb1*::HIS3MX6), which require a plasmid-borne copy of *SPB1* for cell viability, were used in further experiments.

Construction of a *GAL*::*SPB1* allele and *in vivo* depletion of Spb1p

The first 466 nt of the *SPB1* ORF were PCR amplified from plasmid YCplac111-SPB1 (pDK403) with oligonucleotides introducing an in-frame *Sal*I restriction site 5′ of the second codon (ODK120, 5′GCA CGC GTC GAC **GGT** AAG ACA CAA AAG AAG AA-3′, *Sal*I site underlined and the second codon of the *SPB1* ORF in bold type), and 3′ of an internal *Hin*dIII restriction site (ODK121, 5′-CAA AAG TAC CGT TCA CCA CC-3′), respectively. This PCR product was first digested with *Hin*dIII, treated with calf intestinal alkaline phosphatase (Boehringer Mannheim), and then digested with *Sal*I to yield a fragment of 420 nt that was cloned together with a 3.37 kb *Hin*dIII fragment, including the remaining portion of the *SPB1* ORF and 1.27 kb of its 3′ contiguous region, from pDK403 into plasmid pAS24-DBP6 (pDK238) (41) that was first restricted with *Hin*dIII, treated with alkaline phosphatase, and then restricted with *Sal*I. The resulting plasmid, pAS24-SPB1 (pDK376), contains a *GAL1-10* promoter, a start codon followed by a double hemagglutinin epitope tag (HA-tag), and the *SPB1* ORF and its 3′ contiguous region. The *SPB1* ORF sequences originating from the PCR were verified by sequencing. This construct was transformed into strain YDK14-1A pRS416-SPB1. The subsequent counter-selection of pRS416-SPB1 on 5-fluoroorotic acid (5-FOA) plates containing galactose resulted in strain YDK14-1A pAS24-SPB1. Plasmid pAS24-SPB1 complemented the *spb1* null strain to the wild-type extent on medium containing galactose (YPGal) at all the tested temperatures (18, 30 and 37°C). We also refer to this strain as *GAL*::*SPB1* or, if grown in medium containing glucose (YPD), as the Spb1p-depleted strain.

For *in vivo* depletion of Spb1p, YDK14-1A pAS24-SPB1 was grown in liquid YPGal until mid-exponential phase. Cells were harvested, washed and used to inoculate YPD cultures. Cell growth was monitored over a period of 36 h, during which the cultures were regularly diluted into fresh YPD medium to maintain exponential growth. As a control, YDK14-1A YCplac111-SPB1 was used. Samples for western blot analyses, polysome analyses, and RNA extraction were taken at different times.

SPB1 HA epitope tagging and cloning under the control of its cognate promoter

An N-terminally HA-tagged Spb1 fusion protein (HA–Spb1p) was expressed from its cognate promoter at approximately wild-type levels from plasmid YCplac111-HA-SPB1 (pDK423). Plasmid YCplac111-HA-SPB1 was obtained by cloning a 3.64 kb *Nco*I–*Nde*I fragment, the *Nde*I site was blunt ended by T4 DNA polymerase (New England Biolabs) treatment, from pAS24-SPB1 into plasmid pDK425 that was first restricted with *Sac*I, treated with T4 DNA polymerase and then restricted with *Nco*I. Plasmid pDK425 essentially contains the *SPB1* promoter region followed by an *Nco*I restriction site that was introduced at the start codon of *SPB1* by fusion PCR. The correct nature of YCplac111-HA-SPB1 was verified by restriction analysis and by sequencing 170 nt of the promoter region, the double HA tag and the first 750 nt of the *SPB1* ORF. The resulting plasmid, YCplac111-HA-SPB1, complemented the *spb1* null allele almost to the wild-type extent at 30°C. Crude yeast cell extracts were prepared and analyzed by western blotting according to standard procedures (37). Monoclonal 16B12 (BAbCO) and goat anti-mouse alkaline phosphatase-conjugated antibodies (Bio-Rad) were used as primary and secondary antibodies, respectively. The HA-tagged Spb1p was detected as a band that migrated at a molecular mass of ~110 kDa.

Indirect immunofluorescence

Strains YDK14-1A YCplac111-HA-SPB1 and YDK14-1A YCplac111-SPB1 were grown in YPD medium, while strain YDK14-1A pAS24-SPB1 was grown in YPGal medium. In all cases, cultures were grown up to an OD_{600} of ~0.5 and 5 ml of cells were harvested by centrifugation. Preparation of yeast cells for immunofluorescence, immunofluorescence microscopy and image acquisition were done as previously described (25).

Analyses of steady-state levels of ribosomes and pre-rRNAs

Polyribosome and ribosomal subunit preparations and analyses were done exactly as described (42). Gradient analysis was performed using an ISCO UA-6 gradient UV-detection and fraction collection system with continuous monitoring at A_{254}.

Steady-state levels of pre-rRNAs were assessed by northern blot and primer extension analyses according to Venema *et al.* (43). Total RNA was extracted by the acid-phenol method (34) from aliquots of 10 OD_{600} of exponentially growing cells. Oligonucleotides 5′A_0, 18S, D/A_2, A_2/A_3, A_3/B_1, 5.8S, E/C_2, C_1/C_2, 25S (numbered 1–9 according to Fig. 1A) and 5S have been previously described (44). Prior to northern hybridization or primer extension analysis, they were end-labeled with 30 µCi [γ-^{32}P]ATP (5000 Ci/mmol; Amersham) using T4 polynucleotide kinase (Appligene).

Analyses of pre-rRNA methylation

The synthesis, processing and methylation of pre-rRNAs were assayed by pulse–chase analysis with [methyl-^{3}H]methionine, as described by Kressler *et al.* (41). About 250 µCi [methyl-^{3}H]methionine (70–85 Ci/mmol; Amersham) per 40 OD_{600} of yeast cells were used. Total RNA was extracted as described above. Equal amounts of radioactivity (30 000 c.p.m.) were loaded and resolved on 1.2% agarose–6% formaldehyde and 7% polyacrylamide–8 M urea gels and the gels were processed as previously described (42,43).

To assess the steady-state levels of snoRNAs by northern hybridization (43), the oligonucleotides U3 (5′-TTC GGT TTC TCA CTC TGG GGT AC-3′), U14 (5′-GGA ACC AGT CTT TCA TCA CC-3′), U24 (5′-TCA GAG ATC TTG GTG ATA AT-3′), snR10 (5′-CCT TGC AAC GGT CCT CAT CCG GG-3′) and snR190 (5′-CGT CAT GGT CGA ATC GG-3′) were used. Prior to northern hybridization, they were end-labeled with 30 µCi [γ-^{32}P]ATP (5000 Ci/mmol) using T4 polynucleotide kinase.

RESULTS

The *spb1-1* mutant is deficient in 60S ribosomal subunits

The *spb1-1* mutation (mutant strain YAS151) was originally isolated as one of seven different extragenic sg^- and cs^- suppressor mutations of the temperature-sensitive (ts^-) phenotype of a *PAB1* deletion strain (26). It was also shown that the *spb1-1* mutation led to decreased steady-state levels of free

60S ribosomal subunits (26). To use the W303 background and to eliminate undesired second site mutations, the YAS151 strain was back-crossed three times to the W303-derived wild-type strain ASZ1. As expected for *spb1-1* being recessive (26), the heterozygous *spb1-1*/*SPB1* diploid showed wild-type growth. Tetrad analysis of this strain confirmed that the sg$^-$ and cs$^-$ phenotypes segregated 2$^+$:2$^-$ and co-segregated with each other, indicating that both phenotypes were due to a single nuclear mutation. A sg$^-$ and cs$^-$ haploid strain (JDY9-1A) derived from three consecutives crosses with ASZ1 was used to further characterize the *spb1-1* mutation. Sucrose gradient analyses were performed with cell extracts prepared from JDY9-1A and wild-type (CW04) cells grown in YPD at the permissive temperature (30°C). As previously reported (26), when compared with wild-type cells (Fig. 4A), the *spb1-1* mutation led to a deficit of free 60S relative to free 40S ribosomal subunits (Fig. 4B). In addition, it led to an overall decrease in 80S ribosomes (free couples and monosomes) and polysomes, and an accumulation of half-mer polysomes (Fig. 4B). The relative reduction in 60S ribosomal subunits was further analyzed by quantification of total ribosomal subunits in low Mg^{2+} sucrose gradients. An A_{254} 60S:40S ratio of around 2 was obtained for the wild-type strain, whereas this ratio was about 1.4 for strain JDY9-1A. Taken together, polysome and ribosomal subunit analyses indicate that the *spb1-1* mutation results in a deficiency in 60S ribosomal subunits. Therefore, Spb1p plays a role in the metabolism of 60S ribosomal subunits.

SPB1 encodes a putative S-AdoMet-dependent methyltransferase

To isolate the *SPB1* gene, strain JDY9-1A was transformed with a pSEY18-based yeast genomic library and screened for wild-type growth at 30°C. One clone (pSEY18-SPB1) that reproducibly complemented the sg$^-$ phenotype was recovered (Materials and Methods). It comprised a 8.67 kb DNA fragment from chromosome III containing the complete ORFs YCL052C (*PBN1*) and YCL054W. Subcloning into YCplac111 and cloning of the PCR-amplified YCL054W into pRS416 indicated that ORF YCL054W was sufficient to complement the sg$^-$ and cs$^-$ growth phenotypes of the *spb1-1* mutant strain to the wild-type extent.

YCL054W is predicted to encode a basic protein of 841 amino acids (predicted pI 8.08, predicted molecular mass 96.5 kDa). Computational sequence analysis revealed that Spb1p contained an N-terminal S-AdoMet-binding motif (residues 50–58; Fig. 2) characteristic of methyltransferases (45). Contiguous with this motif, we found a conserved post-I methyltransferase motif (residues 74–78; Fig. 2) that is present in a large number of both known and putative methyltransferases (46). Furthermore, at the conserved distance from motif I (46), sequences with a marginal match to the consensus of motifs II and III for methyltransferases was also found (motif II, residues 116–123; motif III, residues 149–158; Fig. 2). Based on these findings, Spb1p can be classified as a putative S-AdoMet-dependent methyltransferase. In addition, Spb1p has a bipartite nuclear targeting sequence (residues 742–758) and a region with a high propensity to form a coiled coil (residues 348–389). Finally, the predicted protein has a high content of charged amino acids (D + E + K + R = 38%), and an acidic and serine-rich stretch at its C-terminus (residues 606–642).

ORF	Protein	Motif I		Post-I		Motif II		Motif III
YBR236c	Abd1p	VLELGCGKG	13	FIGID	46	FPCDIVST	23	SLKIGGHFFG
YOL096c	Coq3p	VLDVGCGGG	14	VQGID	34	GQFDIITC	20	LNPEKGILFL
YML110c	Coq5p	FIDVAGGSG	13	FGDTE	47	DSKDIYTV	19	VLKPGGIFYC
YPL266w	Dim1p	VLEVGPGTG	12	VVAVE	34	PYFDICIS	36	LARPGDSLYC
YML008c	Erg6p	VLDVGCGVG	13	VIGLN	36	NTFDKVYA	19	VLKPGGTFAV
YBR034c	Rmt1p	VLDVGCGTG	13	VIGVD	35	PKVDIIIS	22	YLVEGGLIFP
YKR069w	Met1p	ISLVGSGPG	17	IILAD	51	KQGDPYIF	17	VVLPGISSSL
YCL054W	Spb1p	VIDLCAAPG	15	IIGVD	37	VLHDGAPN	25	NLVVNGTFVT
		50	58	74	78	116	123	149 158

Figure 2. Spb1p is a putative S-AdoMet-dependent methyltransferase. Comparison of the characteristic methyltransferase motifs from seven different known yeast methyltransferases (46) with those found in Spb1p. Numbers between motifs refer to the amino acid residues between two motifs. Numbers below the sequences refer to the amino acid position in Spb1p. Residues of Spb1p that are conserved in one or more of the shown methyltransferases are underlined. Note that the order of motifs as well as their spacing are also conserved.

A database search resulted in the identification of related proteins in *Schizosaccharomyces pombe* (pmt2 methyltransferase, NCBI accession no. CAA22605; 60% similarity, 44% identity over the entire protein) and *Arabidopsis thaliana* (NCBI accession no. CAB39594; 56% similarity, 36% identity over the entire protein). Furthermore, although *SPB1* is a single copy gene in *S.cerevisiae*, a search for proteins homologous to Spb1p at SGD revealed a substantial homology of the N-terminal part of Spb1p with the yeast ORF YBR061C (58% similarity, 43% identity over the first 230 amino acids). Also, the N-terminal part of Spb1p shares significant homology with predicted proteins from *Caenorhabditis elegans* (H06I04.G, Sanger Centre; 60% similarity, 40% identity over the first 316 amino acids) and *Homo sapiens* (AJ005892; 57% similarity, 42% identity over the first 215 amino acids). The strong sequence conservation between species as distant as budding and fission yeasts, *C.elegans*, *A.thaliana* and humans suggests that Spb1p serves an important, evolutionarily conserved function in eukaryotes.

Spb1p is essential for cell viability

As a first approach to the functional analysis of Spb1p, we constructed a *spb1* null allele. We replaced part of one *SPB1* ORF copy in the diploid strain W303 with a HIS3MX6 marker module (strain YDK14; Materials and Methods). Correct gene replacement was verified by Southern blot analysis (data not shown). Tetrad analysis revealed a 2:2 segregation of viable to non-viable spores, with all the viable progeny being auxotrophic for histidine and therefore Spb1$^+$. When YDK14 was transformed with pRS416-SPB1 and subsequently sporulated, complete tetrads could be recovered. All the haploid *spb1*::HIS3MX6 progeny (His$^+$) contained pRS416-SPB1 (Ura$^+$) and were unable to grow on plates containing 5-FOA (data not shown). These results demonstrate that Spb1p is essential for cell viability.

To determine whether YCL054W was indeed the *SPB1* gene, rather than a low copy number suppressor, JDY9-1A was crossed to YDK14-2C pRS416-SPB1 (a *spb1*::HIS3MX6 strain containing a wild-type copy of *SPB1* on a *CEN-URA3* plasmid). After sporulation and tetrad dissection, a 2 His$^+$:2 His$^-$ segregation was obtained. About 20 complete tetrads were tested by counter-selection against the plasmid on plates

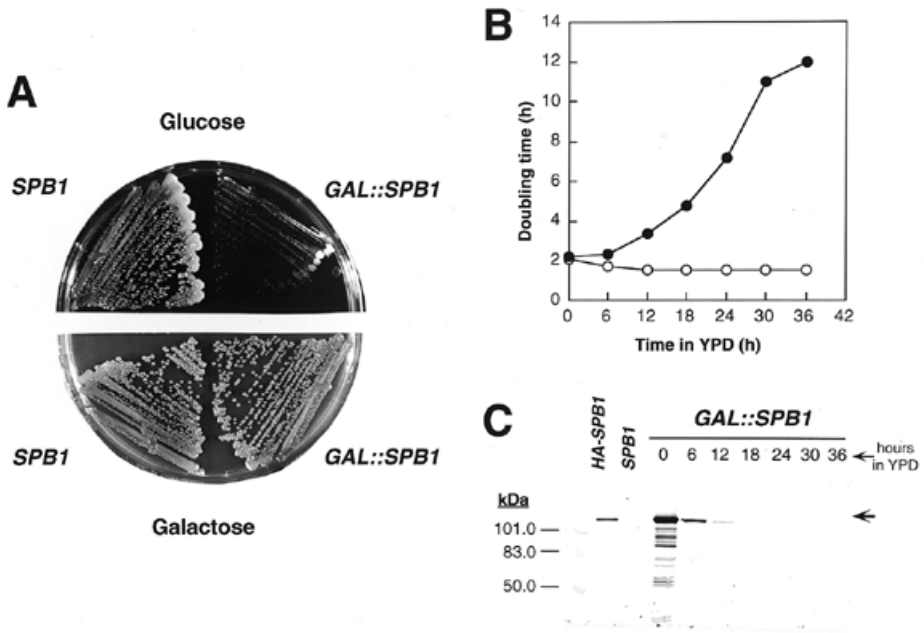

Figure 3. *In vivo* depletion of Spb1p. (**A**) Growth comparison of YDK14-1A pAS24-SPB1 (*GAL*::*SPB1*) and its isogenic counterpart YDK14-1A YCplac111-SPB1 (*SPB1*). Cells were streaked on YPGal (galactose) or YPD (glucose) plates and incubated for 4 days at 30°C. (**B**) Growth curve of YDK14-1A pAS24-SPB1 (*GAL*::*SPB1*, closed circles) and YDK14-1A YCplac111-SPB1 (*SPB1*, open circles) at 30°C after shifting logarithmic cultures from YPGal to YPD for up to 36 h. Data are represented as the doubling time at the different times in YPD. (**C**) Depletion of Spb1p. The strains YDK14-1A YCplac111-SPB1 (*SPB1*) and YDK14-1A pAS24-SPB1 (*GAL*::*SPB1*) were grown in YPGal and shifted to YPD for up to 36 h. YDK14-1A YCplac111-HA-SPB1 (*HA-SPB1*) was directly grown in YPD. Cell extracts were prepared from samples harvested at the indicated times and assayed by western blotting. Equal amounts of total protein (~70 µg) were loaded in each lane, as judged by Coomassie staining of gels or red Ponceau staining of the blots (data not shown). Prestained standards (Bio-Rad) are shown. Monoclonal mouse anti-HA 16B12 antibodies followed by alkaline phosphatase-coupled goat anti-rabbit IgG were used to detect HA–Spb1p. The HA–Spb1p signal is indicated by an arrow. No signal was detected for untagged Spb1p.

containing 5-FOA; two viable sg^- and His^--spore clones were recovered in all cases. All these clones also had a cs^- phenotype. These results indicate that YCL054W is genetically linked to the *SPB1* locus.

Depletion of Spb1p results in a deficit in 60S ribosomal subunits

To better study the function of Spb1p, a different conditional system for phenotypic analysis was established. To this end, the *SPB1* ORF was cloned into pAS24 under the control of an inducible *GAL1-10* promoter, which allows expression of the gene in culture medium that contains galactose (YPGal) but is repressed in culture medium containing glucose (YPD). The resulting plasmid, pAS24-SPB1, expressed an N-terminally HA-tagged Spb1 fusion protein that fully complemented the *spb1* null strain (YDK14-1A) on YPGal and resulted in a severe sg^- phenotype on YPD plates (Fig. 3A). In liquid YPGal medium, there was no difference in the growth rate between the *GAL*::*SPB1* (YDK14-1A pAS24-SPB1) and an isogenic wild-type *SPB1* strain (YDK14-1A YCplac111-SPB1). After transfer of the *GAL*::*SPB1* strain from liquid YPGal to YPD medium, the growth rate progressively decreased to a doubling time of >12 h after 36 h in YPD, as compared to the 1.5 h doubling time for the isogenic *SPB1* strain (Fig. 3B). A concomitant depletion of HA–Spb1p was observed by western blotting (Fig. 3C), as compared to YDK14-1A YCplac111-HA-SPB1, which expresses HA–Spb1p from its cognate promoter (Materials and Methods).

To determine the effects of Spb1p depletion on ribosome metabolism, polysomes were analyzed from the *GAL*::*SPB1* strain following transfer to liquid YPD medium. As shown in Figure 4C, depletion of Spb1p for 6 h already resulted in a deficit of free 60S relative to free 40S ribosomal subunits, an overall decrease in 80S ribosomes (free couples and monosomes), and an accumulation of half-mer polysomes. These features were more pronounced when the *GAL*::*SPB1* strain was transferred to YPD for 24 h (Fig. 4D). Quantification of total ribosomal subunits in low Mg^{2+} sucrose gradients gave an A_{254} 60S:40S ratio of ~1.7 when the *GAL*::*SPB1* strain was transferred to YPD for 6 h. This indicated that the number of total 60S ribosomal subunits was reduced at early times of depletion. Interestingly, the A_{254} 60S:40S ratio increased to ~2.3 when the *GAL*::*SPB1* strain was transferred to YPD for 12 h. After 18 or 24 h in YPD, the overall ribosomal material was strongly decreased and the 40S ribosomal subunit peak was almost absent (data not shown). This observation might therefore reflect an instability of 40S ribosomal subunits at later times of depletion that can only be detected under ribosomal subunit preparation conditions. Altogether, our results indicate that depletion of Spb1p, similarly to the *spb1-1* mutation, leads to a deficiency in 60S ribosomal subunits and therefore that Spb1p plays a role in the metabolism of 60S ribosomal subunits. At

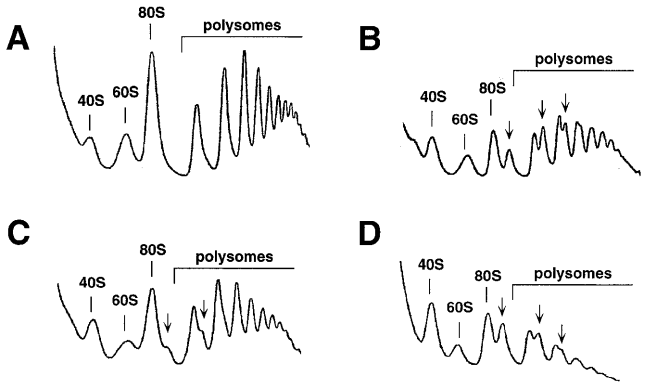

Figure 4. The *spb1-1* mutation and the depletion of Spb1p result in a deficit in free 60S ribosomal subunits and in the accumulation of half-mer polysomes. CW04 (*SPB1*) (**A**) and JDY9-1A (*spb1-1*) (**B**) were grown at 30°C in YPD. YDK14-1A pAS24-SPB1 (*GAL*::*SPB1*) was grown at 30°C in YPGal and shifted to YPD for 6 (**C**) and 24 h (**D**). Cells were harvested at an OD_{600} of 0.8, and cell extracts were resolved in 7–50% sucrose gradients. The A_{254} was continuously measured. Sedimentation is from left to right. The peaks of free 40S and 60S ribosomal subunits, 80S free couples/monosomes and polysomes are indicated. Half-mers are labeled by vertical arrows.

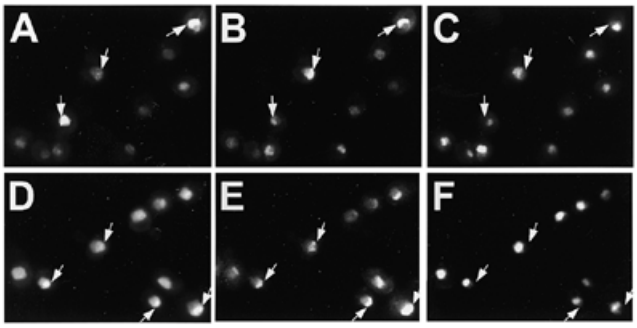

Figure 5. HA–Spb1p localizes to the nucleus with nucleolar enrichment. Indirect immunofluorescence was performed (**A**–**C**) with cells expressing HA–Spb1p from the *SPB1* promoter (YDK14-1A YCplac111-HA-SPB1) or (**D**–**F**) with cells expressing HA–Spb1p from the *GAL1-10* promoter (YDK14-1A pAS24-SPB1). (A and D) HA–Spb1p was detected with the monoclonal mouse anti-HA 16B12 antibody, followed by decoration with a goat anti-mouse rhodamine-conjugated antibody. (B and E) Nop1p was detected with polyclonal rabbit anti-Nop1p antibodies, followed by decoration with a goat anti-rabbit fluorescein-conjugated antibody. (C and F) Chromatin DNA was stained using DAPI. The nucleolar region labeled by Nop1p-specific antibodies (B and E, indicated by arrows) is partially devoid of DAPI stain (C and F, indicated by arrows). Note that Spb1p, which is enriched in the nucleolus (A and D, indicated by arrows), also distributes to the adjacent nucleoplasm.

later times of depletion, the stability of 40S ribosomal subunits is also affected.

Spb1p localizes to the nucleus with nucleolar enrichment

Because most mutants leading to a deficit in 60S ribosomal subunits are either affected in 60S r-proteins or in cytoplasmic, nuclear or nucleolar *trans*-acting factors involved in its biogenesis (25,41,47 and references therein), we determined the subcellular localization of Spb1p by indirect immunofluorescence. For this purpose, *SPB1* was HA-tagged at its 5′-end and cloned into YCplac111 to express the N-terminally epitope-tagged Spb1p (HA–Spb1p) from its cognate promoter at approximately wild-type levels (Materials and Methods). This plasmid (YCplac111-HA-SPB1), or a control plasmid harboring the untagged *SPB1* gene (YCplac111-SPB1), were transformed into strain YDK14-1A pRS416-SPB1. Upon plasmid shuffling and subsequent restreaking on YPD, HA–Spb1p conferred a very weak sg^- phenotype. This slight growth defect (1.9 h doubling time versus 1.5 h for the wild-type strain in liquid YPD at 30°C), which was not observed when HA–Spb1p was overexpressed from pAS24-SPB1 (see above), might reflect a partial loss of HA–Spb1p function due to tagging. Western blot analysis with a monoclonal anti-HA antibody detected a single protein that migrated at a molecular mass of ~110 kDa in a total cell extract from a strain expressing HA–Spb1p (Fig. 3C) but not from a strain expressing untagged Spb1p (Fig. 3C).

Strains YDK14-1A YCplac111-HA-SPB1, YDK14-1A pAS24-SPB1 and YDK14-1A YCplac111-SPB1 were grown in liquid medium and processed for immunofluorescence (Materials and Methods). The HA-tagged Spb1p was detected by anti-HA antibodies, followed by decoration with goat anti-mouse rhodamine-conjugated antibodies (Fig. 5A and D). For precise subnuclear localization, the nucleoplasm was visualized by staining of DNA with 4′,6-diamidino-2-phenylindole dihydrochloride (DAPI) (Fig. 5C and F) and the nucleolus was stained with anti-Nop1p antibodies (48) in combination with goat anti-rabbit fluorescein-conjugated antibodies (Fig. 5B and E). In many cells the anti-Nop1p antibodies gave the crescent-shaped staining characteristic of nucleolar proteins (Fig. 5B and E), which was largely excluded from the DAPI stained area (Fig. 5C and F). When expressed from its cognate promoter, HA–Spb1p localized to the nucleus, where it displayed an uneven distribution that is different from that of DNA stained with DAPI (Fig. 5A and C). In numerous cells the HA–Spb1p signal was enriched in the nucleolus (Fig. 5A; compare with Fig. 5B and C, indicated by arrows), however, this enrichment was less pronounced than that of Nop1p (Fig. 5B). Overexpression of HA–Spb1p resulted in a much stronger signal that was distributed throughout the nucleus with a clear nucleolar enrichment (Fig. 5D; compare with Fig. 5E and F, indicated by arrows). No signal was obtained with the combination of anti-HA and goat anti-mouse rhodamine-conjugated antibodies when cells of strain YDK14-1A YCplac111-SPB1 were analyzed by indirect immunofluorescence (data not shown).

We conclude that Spb1p is a nuclear protein that is enriched in the nucleolus. This result strongly supports a nucleolar function for Spb1p, presumably in 60S ribosomal subunit synthesis.

Spb1p is required for normal pre-rRNA processing

To further characterize the role of Spb1p in 60S ribosomal biogenesis, we assessed the steady-state levels of pre-rRNAs and mature rRNAs. For this purpose, total RNA was isolated from strains YDK14-1A pAS24-SPB1 (*GAL*::*SPB1*) and YDK14-1A YCplac111-SPB1 (*SPB1*) at various time points after a shift from YPGal to YPD. Then, steady-state levels of pre-rRNA intermediates and mature rRNAs were examined by northern blot and primer extension analyses. Specific oligonucleotides hybridizing to defined regions of the 35S pre-rRNA were used to identify the different pre-rRNAs and mature rRNAs (Fig. 1A). As shown in Figure 6A, depletion of Spb1p slightly affected the levels of 18S rRNA, but drastically

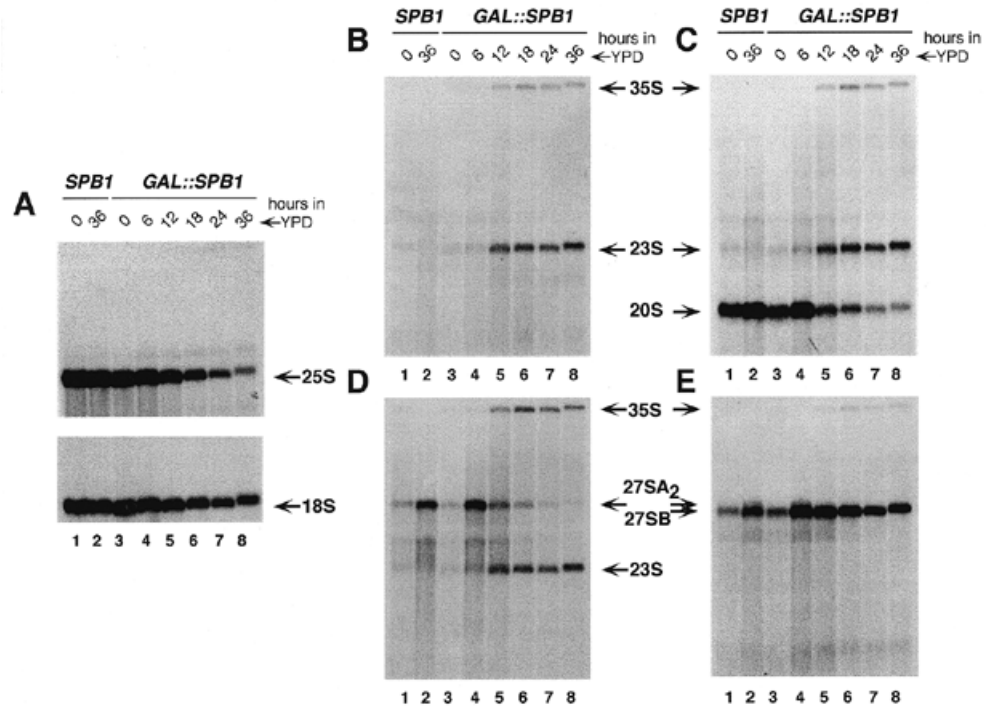

Figure 6. Depletion of Spb1p affects the steady-state levels of pre-rRNA and mature rRNA species. The strains YDK14-1A YCplac111-SPB1 (*SPB1*) and YDK14-1A pAS24-SPB1 (*GAL*::*SPB1*) were grown in YPGal and shifted for up to 36 h to YPD. The cells were harvested at the indicated times and total RNA was extracted. Equal amounts of total RNA (5 µg) were resolved on a 1.2% agarose–6% formaldehyde gel and transferred to a nylon membrane for northern hybridization. The same filter was consecutively hybridized with all the different probes used. (**A**) Hybridization with probes 2 and 9 (see Fig. 1A for location of the probes), base pairing to sequences within the mature 18S and 25S rRNAs, respectively; (**B**) probe 1 in the 5′-ETS; (**C**) probe 3 in ITS1, between sites D and A_2; (**D**) probe 4 in ITS1, between sites A_2 and A_3; (**E**) probe 8 in ITS2, between sites C_2 and C_1. The positions of the different pre-rRNAs and mature rRNAs are indicated by arrows.

decreased the levels of 25S rRNA. These data show that Spb1p is mainly required for accumulation of 25S rRNA. Nevertheless, and in agreement with delayed cleavage at sites A_0, A_1 and A_2 (7), depletion of Spb1p resulted in a notable decrease in the levels of 20S rRNA (Fig. 6C), and in a more drastic decrease in the $27SA_2$ pre-rRNA (Fig. 6D). Concomitantly, the 35S pre-rRNA accumulated slightly (Fig. 6B–E), and the well-characterized aberrant 23S pre-rRNA species (7) appeared (Fig. 6B–D). Most importantly, a significant accumulation of the 27SB pre-rRNAs was observed, commencing early upon transfer to YPD (Fig. 6E, lanes 4–8). Analysis of low molecular weight rRNA species revealed a significant depletion of the 7S pre-rRNA (Fig. 7, top) and a slight decrease in mature 5.8S rRNAs (Fig. 7, bottom). Neither the ratio of $5.8S_S$ and $5.8S_L$ rRNAs nor the steady-state levels of the 5S rRNA were affected by Spb1p depletion (Fig. 7, bottom).

Because northern hybridization does not distinguish between the $27SA_2$ and $27SA_3$, and between the $27SB_L$ and $27SB_S$ precursors, we assessed the levels of these species by primer extension analyses, using oligonucleotides 5 and 8 as primers (Fig. 1A). The level of the primer extension stop at site A_2, the 5′-end of the $27SA_2$ pre-rRNA, was substantially reduced upon depletion of Spb1p (Fig. 8, top), which is fully consistent with the results obtained by northern hybridization. The level of the $27SA_3$ pre-rRNA, as shown by the stop at site A_3, notably increased at 6 and 12 h after transfer to glucose and then progressively decreased to wild-type levels (Fig. 8, middle).

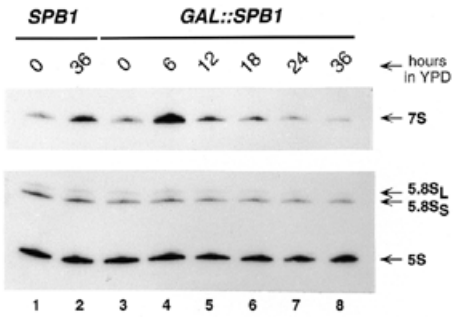

Figure 7. Spb1p depletion leads to lower steady-state levels of the 7S precursor and the mature 5.8S rRNAs. The strains YDK14-1A YCplac111-*SPB1* (*SPB1*) and YDK14-1A pAS24-*SPB1* (*GAL*::*SPB1*) were grown in YPGal and shifted for up to 36 h to YPD. The cells were harvested at the indicated times. Total RNA was extracted, separated on a 7% polyacrylamide–8 M urea gel, transferred to a nylon membrane, and subjected to northern analysis. The same filter was consecutively hybridized with the three different probes: oligonucleotide 7 in ITS2 between sites E and C_2 (top); oligonucleotide 6, base pairing to sequences within the mature 5.8S rRNAs (bottom); oligonucleotide 5S, base pairing to sequences within the mature 5S rRNAs (bottom). The positions of the 7S pre-rRNA and the mature 5.8S and 5S rRNAs are indicated.

Most importantly, the primer extension stops at sites B_{1L} and B_{1S} increased at 12 h and later times after transfer to glucose medium (Fig. 8, bottom), indicating that both $27SB_L$ and $27SB_S$ accumulated upon depletion of Spb1p. Finally, primer

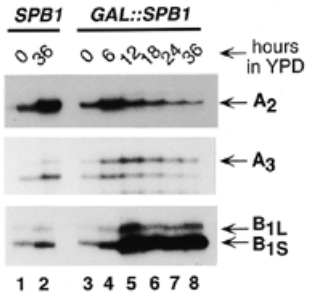

Figure 8. Depletion of Spb1p leads to higher steady-state levels of the 27SB precursors. The strains YDK14-1A YCplac111-SPB1 (*SPB1*) and YDK14-1A pAS24-SPB1 (*GAL*::*SPB1*) were grown in YPGal and shifted for up to 36 h to YPD. The cells were harvested at the indicated times and total RNA was extracted. Primer extension with oligonucleotide 8 within ITS2 reveals the processing sites B_{1S}, B_{1L} (bottom), and A_2 (top). The middle panel corresponds to a primer extension with oligonucleotide 5, priming 3′ to site A_3, and reveals processing at this site. Arrows indicate the positions of the primer extension stops corresponding to the different pre-rRNA species analyzed.

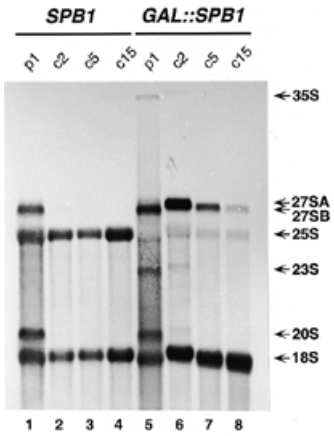

Figure 9. Global methylation is not affected upon depletion of Spb1p. The wild-type control strain YDK14-1A YCplac111-*SPB1* (*SPB1*) and strain YDK14-1A pAS24-*SPB1* (*GAL*::*SPB1*) were grown at 30°C in YPGal, and then shifted for 22 h to SD-Met. Cells were pulse-labeled for 1 min with [methyl-^{3}H]methionine and then chased for 2, 5 and 15 min with an excess of unlabeled methionine. Total RNA was extracted and 30 000 c.p.m. was loaded and separated on a 1.2% agarose–6% formaldehyde gel, transferred to a nylon membrane, and visualized by fluorography. The positions of the different pre-rRNAs and mature rRNAs are indicated.

extension analysis also showed that processing at all these sites was accurate at the nucleotide level during the time course of Spb1p depletion.

Altogether, our results indicate that the formation of mature 25S and 5.8S rRNAs is impaired upon depletion of Spb1p. This is mainly due to inhibition of processing of the 27SB pre-rRNAs at sites C_1 and C_2. As a consequence of this inhibition, 27SB pre-rRNAs accumulate, and the steady-state levels of 7S pre-rRNA and mature 25S and 5.8S rRNAs decrease. The pre-rRNA cleavages at sites A_0, A_1 and A_2 are delayed upon Spb1p depletion, as evidenced by the slight increase in 35S pre-rRNA and the decreased steady-state levels of the 27SA and 20S pre-rRNAs. However, the levels of mature 18S rRNA only slightly decrease. On the basis of these results, the 60S ribosomal subunit deficiency upon Spb1p depletion and the predominant nucleolar localization of HA–Spb1p, we conclude that Spb1p has a role in 60S ribosomal subunit biogenesis.

Global methylation of pre-rRNAs is not affected upon depletion of Spb1p

Because the putative S-AdoMet-dependent methyltransferase Spb1p is involved in 60S ribosomal subunit biogenesis, we determined if Spb1p could be required for pre-rRNA methylation. For this purpose, we analyzed the effects of depleting Spb1p on the global methylation of pre-rRNAs by [methyl-^{3}H]-methionine pulse–chase labeling experiments (Fig. 9 and its legend). In the wild-type *SPB1* strain, the 35S precursor was very rapidly processed into 32S pre-rRNA and then into 27S and 20S species, the immediate precursors of the mature 25S and the 18S rRNA, respectively (Fig. 9, lanes 1–4). In the Spb1p-depleted strain, we observed that processing of the 35S precursor was delayed (Fig. 9, lanes 5 and 6). Consistent with the northern blot and primer extension results, the 27SB precursors persisted beyond the 15 min chase time point (Fig. 9, lanes 5–8). As a consequence, almost no labeled mature 25S rRNA was detected (Fig. 9, lane 8). The processing pathway leading to the formation of 18S rRNA was not significantly affected, as revealed by similar kinetics of processing of the 20S precursor to the mature 18S rRNA, and the similar levels of mature 18S rRNA in both the Spb1p-depleted and the wild-type strain (Fig. 9). Nevertheless, the aberrant 23S species was detected (Fig. 9, lanes 5 and 6), which is indicative of delayed processing at sites A_0–A_2 (7). Altogether, these results confirmed that the deficit in 60S ribosomal subunits following Spb1p depletion was due to inhibition of processing of the 27SB precursors to mature 25S (and 5.8S) rRNAs.

The incorporation of tritiated methionine into pre-rRNAs and mature 18S rRNA was comparable in wild-type and Spb1p-depleted cells (Fig. 9). Synthesis and methylation of tRNAs were also similar in wild-type cells and upon depletion of Spb1p, as revealed by the analysis of these labeled RNAs by polyacrylamide gel electrophoresis (data not shown). These results, therefore, argue against a global impairment of pre-rRNA methylation (2′-*O*-ribose methylation and base methylation) following Spb1p depletion. However, we cannot exclude the possibility that Spb1p is required for 2′-*O*-ribose or base methylation of specific positions within pre-rRNAs. Recently, it has been described that Nop58p, Nop56p and Nop1p form the core of all C/D-box snoRNPs (49–52; D.Lafontaine and D.Tollervey, personal communication); most of the C/D-box snoRNPs are required for 2′-*O*-ribose methylation of pre-rRNAs (18,53). Depletion of Nop58p results in the inhibition of pre-rRNA processing at sites A_0 and A_2, and the instability of all C/D-box snoRNAs (50). Surprisingly, global methylation is not affected upon Nop58p depletion (50,52). To test whether Spb1p was required for stability of the C/D-box snoRNAs, steady-state levels of several snoRNAs were assessed by northern blotting following Spb1p depletion (Materials and Methods). Normal steady-state levels for all the tested C/D-box (U14, U3, U24 and snR190) and H/ACA-box (snR10) snoRNAs were observed (data not shown). Additionally, the steady-state level of Nop1p was not affected by depletion of Spb1p (data not shown).

DISCUSSION

In this paper, we describe the identification and the functional characterization of Spb1p, an essential putative S-AdoMet-dependent methyltransferase. Polysome analysis and quantification of total ribosomal subunits in the *spb1-1* and *GAL*::*SPB1* strains revealed a deficit in 60S ribosomal subunits leading to the appearance of half-mer polysomes. Similar profiles have been described for mutants defective in 60S r-proteins or in *trans*-acting factors involved in their biogenesis (25,41,47 and references therein). Since we found that an N-terminally HA-tagged Spb1p localizes to the nucleus and is enriched in the nucleolus, we conclude that Spb1p is not a structural component of 60S ribosomal subunits but rather plays a role in their biogenesis. Consistent with this, northern blotting, primer extension and pulse–chase labeling of pre-rRNAs and mature rRNAs revealed that the deficit in 60S ribosomal subunits in the *GAL*::*SPB1* strain is a consequence of inhibition of normal pre-rRNA processing, which causes an under-accumulation of mature 25S and 5.8S rRNAs. Processing of the 35S precursor at sites A_0, A_1 and A_2 (Fig. 1) was slightly delayed upon Spb1p depletion, as revealed by appearance of the aberrant 23S pre-rRNA species and by lower levels of the 27SA and 20S precursors. Most importantly, the processing of $27SB_L$ and $27SB_S$ pre-rRNAs to mature 25S and 5.8S rRNAs was strongly inhibited, and therefore the Spb1p-depleted strain substantially accumulated 27SB pre-rRNAs, as revealed by northern and primer extension analyses. Nevertheless, processing was still accurate at the nucleotide level and no aberrant precursor in the 25S and 5.8S rRNA pathway was observed. Moreover, the 27SB precursors are relatively stable upon Spb1p depletion, as revealed by pulse–chase analysis. We conclude that normal processing of 27SB pre-rRNAs requires Spb1p.

Many protein *trans*-acting factors have been described as participating in 60S ribosomal subunit biogenesis (7–12). Based on the fate of the 27S pre-rRNAs upon mutation in or depletion of any of these factors, they can be grouped into two classes. Mutation in or depletion of protein *trans*-acting factors belonging to the first class lead to abortive assembly of pre-60S ribosomal particles, resulting in the destabilization of 27S pre-rRNA intermediates (see for example 41 and references therein). Mutation in or depletion of the factors of the second class lead to the accumulation of pre-60S ribosomal particles (arrested assembly) and stabilization of 27S pre-rRNAs (see below for examples). The phenotype observed after depletion of Spb1p closely resembles that described for Nip7p, Nop2p, Nop3p and Spb4p (25,54–56). Delayed conversion of 27SB pre-rRNA to mature 25S rRNA and accumulation of 27SB pre-rRNAs is seen upon depletion of any of these factors. Interestingly, Spb1p depletion results primarily in a deficit in 60S ribosomes but also affects the stability of 40S ribosomal subunits. Thus, it can be speculated that Spb1p associates with the pre-ribosomes at an early stage before separation into 66S and 43S particles, which are the direct precursors of the 60S and 40S ribosomal subunits, respectively. The inhibition of 27SB processing observed upon Spb1p depletion could be explained by an improper early assembly of pre-ribosomal particles during the biogenesis of 60S ribosomal subunits. Similarly, depletion of Cbf5p, the putative rRNA Ψ-synthase, leads to a strong delay in the processing of the 27SB and 7S pre-rRNAs. Although Ψ formation occurs on the primary pre-rRNA transcript and is therefore a very early event during ribosome biogenesis (57), the above phenotype might also be an indirect consequence of perturbing the assembly of 60S ribosomal subunits at an early stage.

Sequence analyses suggest that Spb1p is an S-AdoMet-dependent methyltransferase. Although we have not identified the potential substrates of Spb1p, its nucleolar localization and its requirement for 60S ribosomal biogenesis raise the possibility that Spb1p is a rRNA methyltransferase. If this is the case, Spb1p might methylate a subset of residues within the pre-rRNAs, since global methylation of pre-rRNAs (2′-*O*-ribose methylation and base methylation) is not affected upon Spb1p depletion. Global methylation of pre-rRNAs is neither affected in the *spb1-1* and ts⁻ *spb1-2* (also *ycl54-1*; 30) mutants at the permissive temperature nor in the *spb1-2* mutant after a shift for 1 h to the restrictive temperature (L.Pintard and B.Lapeyre, personal communication). Our results, however, do not discount the possibility that Spb1p depletion may be sufficient to affect 60S ribosomal biogenesis but not the methylation of pre-rRNAs. A similar scenario has recently been described for the depletion of Nop58p (50). Depletion of Nop58p results in instability of all C/D-box snoRNAs, and consistent with this, in inhibition of pre-rRNA processing at sites A_0, A_1 and A_2 (50). However, overall 2′-*O*-ribose methylation is not affected upon Nop58p depletion (50). Dim1p, Ncl1p and Nop2p are other putative S-AdoMet-dependent methyltransferases, which have been previously described to participate in the biogenesis or function of cytoplasmic ribosomes (21,22,55,58). Nop1p, a core protein of all C/D-box snoRNPs (49), is the only protein so far described to be required for overall 2′-*O*-methylation (59,60). Interestingly, Nop1p has recently been identified as a member of a family of putative S-AdoMet-dependent methyltransferases (46). Therefore, it cannot be excluded that Nop1p itself may be a major rRNA 2′-*O*-ribose methyltransferase. 2′-*O*-Ribose methylation at a specific site in the 27S pre-rRNA ($UmGm\Psi UC_{2922}$) is delayed upon Nop2p depletion (55). Dim1p is responsible for the only base methylation studied in yeast so far, the evolutionarily conserved dimethylation of two adjacent adenosines ($m^{6,2}A_{1779}$ and $m^{6,2}A_{1780}$) at the 3′-end of 18S rRNA (21). Dim1p is also required for pre-rRNA processing at sites A_1 and A_2 (22). Since dimethylation occurs on the 20S pre-rRNA (22), which is consistent with earlier reports that formation of $m^{6,2}A{\cdot}m^{6,2}A$ is a late event in ribosome synthesis (61), it can be concluded that processing at sites A_1 and A_2 does not require prior dimethylation. In agreement with this, the ts⁻ *dim1-2* mutation strongly inhibits dimethylation, while pre-rRNA processing is practically unaffected at the permissive temperature (23). Most importantly, pre-rRNA processing is insensitive to ts⁻ mutations in or depletion of Dim1p, when transcription of the rDNA unit is driven by the RNA pol II *PGK* promoter (23). This strongly suggests that Dim1p is only 'physically' required for pre-rRNA processing in the normal scenario, when the rDNA unit is transcribed by RNA pol I. It has been speculated that Dim1p binds to pre-ribosomes at an early stage, and an unknown component senses the correct association of Dim1p within these pre-ribosomes. In the absence of binding of Dim1p, pre-rRNA processing at sites A_1 and A_2 is blocked as a way of preventing the formation of unmodified 18S pre-rRNA. This 'quality control mechanism', however, does not operate when the rDNA is transcribed by RNA pol II from the *PGK* promoter (further discussed in 23,62). Further experiments should allow

us to provide evidence as to whether a similar mechanism exists for 60S ribosomal subunit biogenesis in the absence of putative rRNA methyltransferases such as Nop2p or Spb1p.

ACKNOWLEDGEMENTS

We thank M. Doère for technical assistance and E. C. Hurt for the kind gift of the anti-Nop1p antibodies. We particularly thank A. Sachs for providing strain YAS151 and M. Hall for providing the pSEY18-based yeast genomic library. We also thank L. Pintard and B. Lapeyre for communicating results prior to publication. We are grateful to D. Tollervey, J. Venema and members of our laboratory for fruitful discussions, and F. Shewmaker for critical reading of the manuscript. We gratefully acknowledge C. Georgopoulos for support. J.d.l.C. especially thanks A. Vioque for encouragement. J.d.l.C. was a recipient of fellowships from the Spanish Government (MEC), Sandoz-Stiftung and Ciba-Geigy Jubiläums-Stiftung. This work was funded by grants from the Swiss National Science Foundation and the University of Geneva to P.L.

REFERENCES

1. Mélèse,T. and Xue,Z. (1995) *Curr. Opin. Cell Biol.*, **7**, 319–324.
2. Scheer,U. and Hock,R. (1999) *Curr. Opin. Cell Biol.*, **11**, 385–390.
3. Woolford,J.L.,Jr and Warner,J.R. (1991) In Broach,J.R., Pringle,J.R. and Jones,E.W. (eds), *The Molecular and Cellular Biology of the Yeast Saccharomyces: Genome Dynamics, Protein Synthesis and Energetics*. Cold Spring Harbor Laboratory Press, Cold Spring Harbor, NY, Vol. 1, pp. 587–626.
4. Raué,H.A. and Planta,R.J. (1991) *Prog. Nucleic Acid Res. Mol. Biol.*, **41**, 89–129.
5. Eichler,D.C. and Craig,N. (1994) *Prog. Nucleic Acid Res. Mol. Biol.*, **49**, 197–239.
6. Planta,R.J. (1997) *Yeast*, **13**, 1505–1518.
7. Venema,J. and Tollervey,D. (1995) *Yeast*, **11**, 1629–1650.
8. Lafontaine,D. and Tollervey,D. (1995) *Biochem. Cell Biol.*, **73**, 803–812.
9. Tollervey,D. (1996) *Exp. Cell Res.*, **229**, 226–232.
10. de la Cruz,J., Kressler,D. and Linder,P. (1999) *Trends Biochem. Sci.*, **24**, 192–198.
11. Venema,J. and Tollervey,D. (1999) *Annu. Rev. Genet.*, in press.
12. Kressler,D., Linder,P. and de la Cruz,J. (1999) *Mol. Cell. Biol.*, in press.
13. Ofengand,J. and Fournier,M.J. (1998) In Grosjean,H. and Benne,R. (eds), *Modification and Editing of RNA*. ASM Press, Washington, DC, pp. 229–253.
14. Maden,B.E.H. and Hughes,J.M.X. (1997) *Chromosoma*, **105**, 391–400.
15. Bachellerie,J.-P. and Cavaillé,J. (1998) In Grosjean,H. and Benne,R. (eds), *Modification and Editing of RNA*. ASM Press, Washington, DC, pp. 255–272.
16. Ganot,P., Bortolin,M.-L. and Kiss,T. (1997) *Cell*, **89**, 799–809.
17. Ni,J., Tien,A.L. and Fournier,M.J. (1997) *Cell*, **89**, 565–573.
18. Kiss-László,Z., Henry,Y., Bachellerie,J.-P., Caizergues-Ferrer,M. and Kiss,T. (1996) *Cell*, **85**, 1077–1088.
19. Lafontaine,D.L.J., Bousquet-Antonelli,C., Henry,Y., Caizergues-Ferrer,M. and Tollervey,D. (1998) *Genes Dev.*, **12**, 527–537.
20. Watkins,N.J., Gottschalk,A., Neubauer,G., Kastner,B., Fabrizio,P., Mann,M. and Lührmann,R. (1998) *RNA*, **4**, 1549–1568.
21. Lafontaine,D., Delcour,J., Glasser,A.-L., Desgrès,J. and Vandenhaute,J. (1994) *J. Mol. Biol.*, **241**, 492–497.
22. Lafontaine,D., Vandenhaute,J. and Tollervey,D. (1995) *Genes Dev.*, **9**, 2470–2481.
23. Lafontaine,D.L.J., Preiss,T. and Tollervey,D. (1998) *Mol. Cell. Biol.*, **18**, 2360–2370.
24. Trapman,J., Retèl,J. and Planta,R.J. (1975) *Exp. Cell Res.*, **90**, 95–104.
25. de la Cruz,J., Kressler,D., Rojo,M., Tollervey,D. and Linder,P. (1998) *RNA*, **4**, 1268–1281.
26. Sachs,A.B. and Davis,R.W. (1989) *Cell*, **58**, 857–867.
27. Boeck,R., Lapeyre,B., Brown,C.E. and Sachs,A.B. (1998) *Mol. Cell. Biol.*, **18**, 5062–5072.
28. Mangus,D.A., Amrani,N. and Jacobson,A. (1998) *Mol. Cell. Biol.*, **18**, 7383–7396.
29. Sachs,A.B. and Davis,R.W. (1990) *Science*, **247**, 1077–1079.
30. Loo,S., Laurenson,P., Foss,M., Dillin,A. and Rine,J. (1995) *Genetics*, **141**, 889–902.
31. Thomas,B.J. and Rothstein,R. (1989) *Cell*, **56**, 619–630.
32. Coppolecchia,R., Buser,P., Stotz,A. and Linder,P. (1993) *EMBO J.*, **12**, 4005–4011.
33. Kaiser,C., Michaelis,S. and Mitchell,A. (1994) *Methods in Yeast Genetics: A Cold Spring Harbor Laboratory Course Manual*. Cold Spring Harbor Laboratory Press, Cold Spring Harbor, NY.
34. Ausubel,F.M., Brent,R., Kingston,R.E., Moore,D.D., Seidman,J.G., Smith,J.A. and Struhl,K. (1994) *Current Protocols in Molecular Biology*. John Wiley & Sons, New York, NY, Vol. 2, pp. 13.0.1–13.14.17.
35. Gietz,D., St Jean,A., Woods,R.A. and Schiestl,R.H. (1992) *Nucleic Acids Res.*, **20**, 1425.
36. Wach,A., Brachat,A., Alberti-Segui,C., Rebischung,C. and Philippsen,P. (1997) *Yeast*, **13**, 1065–1075.
37. Sambrook,J., Fritsch,E.F. and Maniatis,T. (1989) *Molecular Cloning: A Laboratory Manual*, 2nd Edn. Cold Spring Harbor Laboratory Press, Cold Spring Harbor, NY.
38. Ward,A. (1990) *Nucleic Acids Res.*, **18**, 5319.
39. Gietz,R.D. and Sugino,A. (1988) *Gene*, **74**, 527–534.
40. Sikorski,R.S. and Hieter,P. (1989) *Genetics*, **122**, 19–27.
41. Kressler,D., de la Cruz,J., Rojo,M. and Linder,P. (1998) *Mol. Cell. Biol.*, **18**, 1855–1865.
42. Kressler,D., de la Cruz,J., Rojo,M. and Linder,P. (1997) *Mol. Cell. Biol.*, **17**, 7283–7294.
43. Venema,J., Planta,R.J. and Raué,H.A. (1998) In Martin,R. (ed.), *Protein Synthesis: Methods and Protocols*. Humana Press, Totowa, NJ, Vol. 77, pp. 257–270.
44. de la Cruz,J., Kressler,D., Tollervey,D. and Linder,P. (1998) *EMBO J.*, **17**, 1128–1140.
45. Koonin,E.V. (1994) *Nucleic Acids Res.*, **22**, 2476–2478.
46. Niewmierzycka,A. and Clarke,S. (1999) *J. Biol. Chem.*, **274**, 814–824.
47. Ho,J.H.-N. and Johnson,A.W. (1999) *Mol. Cell. Biol.*, **19**, 2389–2399.
48. Schimmang,T., Tollervey,D., Kern,H., Frank,R. and Hurt,E.C. (1989) *EMBO J.*, **8**, 4015–4024.
49. Ganot,P., Caizergues-Ferrer,M. and Kiss,T. (1997) *Genes Dev.*, **11**, 941–956.
50. Lafontaine,D.L.J. and Tollervey,D. (1999) *RNA*, **5**, 455–467.
51. Gautier,T., Bergès,T., Tollervey,D. and Hurt,E. (1997) *Mol. Cell. Biol.*, **17**, 7088–7098.
52. Wu,P., Brockenbrough,J.S., Metcalfe,A.C., Chen,S. and Aris,J.P. (1998) *J. Biol. Chem.*, **273**, 16453–16463.
53. Lowe,T.M. and Eddy,S.R. (1999) *Science*, **283**, 1168–1171.
54. Zanchin,N.I.T., Roberts,P., DeSilva,A., Sherman,F. and Goldfarb,D.S. (1997) *Mol. Cell. Biol.*, **17**, 5001–5015.
55. Hong,B., Brockenbrough,J.S., Wu,P. and Aris,J.P. (1997) *Mol. Cell. Biol.*, **17**, 378–388.
56. Russell,I.D. and Tollervey,D. (1992) *J. Cell Biol.*, **119**, 737–747.
57. Brand,R.C., Klootwijk,J., Sibum,C.P. and Planta,R.J. (1979) *Nucleic Acids Res.*, **7**, 121–134.
58. Wu,P., Brockenbrough,J.S., Paddy,M.R. and Aris,J.P. (1998) *Gene*, **220**, 109–117.
59. Tollervey,D., Lehtonen,H., Carmo-Fonseca,M. and Hurt,E.C. (1991) *EMBO J.*, **10**, 573–583.
60. Tollervey,D., Lehtonen,H., Jansen,R., Kern,H. and Hurt,E.C. (1993) *Cell*, **72**, 443–457.
61. Brand,R.C., Klootwijk,J., van Steenbergen,T.J.M., de Kok,A.J. and Planta,R.J. (1977) *Eur. J. Biochem.*, **75**, 311–318.
62. Lafontaine,D.L.J. and Tollervey,D. (1998) In Grosjean,H. and Benne,R. (eds), *Modification and Editing of RNA*. ASM Press, Washington, DC, pp. 281–288.
63. Sun,C. and Woolford,J.L.,Jr (1994) *EMBO J.*, **13**, 3127–3135.
64. Bergès,T., Petfalski,E., Tollervey,D. and Hurt,E.C. (1994) *EMBO J.*, **13**, 3136–3148.
65. Zanchin,N.I.T. and Goldfarb,D.S. (1999) *Mol. Cell. Biol.*, **19**, 1518–1525.